ISSN 1674-1056
http://cpb.iphy.ac.cn
http://iopscience.iop.org/cpb
中国物理 B
Chinese Physics
中国物理 Chinese Physics B

Effect of annealing temperature on coercivity of Nd-Fe-B magnets with TbFeAl doping by process of hot-pressing

Ze-Teng Shu(舒泽腾), Bo Zheng(郑波), Guang-Fei Ding(丁广飞), Shi-Cong Liao(廖是聪), Jing-Hui Di(邸敬慧), Shuai Guo(郭帅), Ren-Jie Chen(陈仁杰), A-Ru Yan(闫阿儒), Lei Shi(石磊)
Citation: Chin. Phys. B . 2020, 29(5): 057501 . **doi:** 10.1088/1674-1056/ab7b57
Journal homepage: http://cpb.iphy.ac.cn; http://iopscience.iop.org/cpb

What follows is a list of articles you may be interested in

Thermal stability, crystallization, and magnetic properties of FeNiBCuNb alloys

Zhe Chen(陈哲), Qian-Ke Zhu(朱乾科), Shu-Ling Zhang(张树玲), Ke-Wei Zhang(张克维), Yong Jiang(姜勇)
Chin. Phys. B . 2019, 28(8): 087502 . **doi:** 10.1088/1674-1056/28/8/087502

Grain boundary restructuring and La/Ce/Y application in Nd-Fe-B magnets

Mi Yan(严密), Jiaying Jin(金佳莹), Tianyu Ma(马天宇)
Chin. Phys. B . 2019, 28(7): 077507 . **doi:** 10.1088/1674-1056/28/7/077507

Coercivity mechanisms in nanostructured permanent magnets

G P Zhao(赵国平), L Zhao(赵莉), L C Shen(沈来川), J Zou(邹静), L Qiu(邱雷)
Chin. Phys. B . 2019, 28(7): 077505 . **doi:** 10.1088/1674-1056/28/7/077505

Regulating element distribution to improve magnetic properties of sintered Nd-Fe-B/Tb-Fe-B composite magnets

Zhu-Bai Li(李柱柏), Jing-Yan Zuo(左敬燕), Dong-Shan Wang(王东山), Fei Liu(刘飞), Xue-Feng Zhang(张雪峰)
Chin. Phys. B . 2019, 28(7): 077503 . **doi:** 10.1088/1674-1056/28/7/077503

Micromagnetic simulations of reversal magnetization in cerium-containing magnets

Lei Li(李磊), Shengzhi Dong(董生智), Hongsheng Chen(陈红升), Ruijiao Jiang(姜瑞姣), Dong Li(李栋), Rui Han(韩瑞), Dong Zhou(周栋), Minggang Zhu(朱明刚), Wei Li(李卫), Wei Sun(孙威)
Chin. Phys. B . 2019, 28(3): 037502 . **doi:** 10.1088/1674-1056/28/3/037502

Effect of annealing temperature on coercivity of Nd–Fe–B magnets with TbFeAl doping by process of hot-pressing*

Ze-Teng Shu(舒泽腾)[1,2], Bo Zheng(郑波)[2,†], Guang-Fei Ding(丁广飞)[2], Shi-Cong Liao(廖是聪)[2], Jing-Hui Di(邸敬慧)[2], Shuai Guo(郭帅)[2,‡], Ren-Jie Chen(陈仁杰)[2], A-Ru Yan(闫阿儒)[2], and Lei Shi(石磊)[1]

[1] *Nano Science and Technology Institute, University of Science and Technology of China, Suzhou* 215123, *China*

[2] *Chinese Academy of Sciences Key Laboratory of Magnetic Materials and Devices, Ningbo Institute of Materials Technology and Engineering, Chinese Academy of Sciences, Ningbo* 315201, *China*

(Received 9 January 2020; revised manuscript received 26 January 2020; accepted manuscript online 1 March 2020)

The Nd–Fe–B magnets are pre-sintered and then processed with hot-pressing, and the resulting magnets are called the hot-pressed pretreated (HPP) magnets. The coercivity of the HPP magnets increases as the annealed temperature increases. When the annealing temperature is 900 °C, the coercivity of the magnet is only 17.6 kOe (1 Oe = 79.5775 A·m^{-1}), but when the annealing temperature rises up to 1060 °C, the coercivity of the magnet reaches 23.53 kOe, which is remarkably increased by 33.7%. The microstructure analysis indicates that the grain surface of the HPP magnet becomes smoother as the annealed temperature increases. The microstructure factor α is changed according to the intrinsic coercivity model formula. The α of the magnet at 900 °C is only 0.578, but it is 0.825 at 1060 °C. Microstructural optimization is due mainly to the increase of coercivity of the HPP magnet.

Keywords: hot-pressed, coercivity, microstructure, anisotropy field

PACS: 75.60.Nt, 75.50.Ww, 75.50.Vv, 75.60.Ej **DOI:** 10.1088/1674-1056/ab7b57

1. Introduction

Recently, high-performance Nd–Fe–B sintered magnets are widely applied to traction motors of electric vehicles and hybrid electric vehicles.[1] Owing to the fact that the Nd–Fe–B magnets are used more and more, it is necessary to reduce the Nd–Fe–B cost by using a few heavy rare earth (HRE) elements (*e.g.*, Tb and Dy) in production. At present, there are two methods of reducing the use of the HRE elements in Nd–Fe–B factory. One method is the grain boundary diffusion (GBD) method by precipitating the HRE compound on the surface of the magnet.[2–4] In the suitable heat treatment process, the HRE element diffuses from the surface along the grain boundary to the inside of the magnet, so that the HRE element mainly exists at the grain boundary and the periphery of the grain. The HRE element does not entry into the interior of the grains too much, which will form the relatively uniform core-shell structure. The existence of the hard $(HRE,Nd)_2Fe_{14}B$ shell can effectively inhibit the reverse nucleation of magnetic domains.[5,6] Therefore, the shell structure having a high magnetocrystalline anisotropy field is formed, which can greatly increase the H_{cj}[7] and thus improve the thermal stability of magnet byless reducing B_r value.[8,9] The H_{cj} of the magnet decreases with increasing magnet thickness due to the limited diffusion depth of HRE in the GBD magnet.[10]

The othermethod is the dual-alloy method by mixing Nd–Fe–B powders and additive powders containing HREs, and the magnets are prepared by magnetic field orientation, molding, and sintering.[11] In the sintering process, the main phase grains of the sintered magnets and the small grains will dissolve, which will precipitate on the grain surface in the cooling process. Due to the high sintering temperature, the atomic motion is so intense that HRE elements are more likely to displace Nd of the main phase grains. Hence, some grains of the dual-alloy magnets do not form the core–shell structure and other grains form the thick core–shell structure, which is disadvantageous for the large increase of H_{cj}.[12]

In order to make the core–shell structure of the dual-alloy magnet relatively uniform, we have improved the traditional dual-alloy process: the dual-alloy powders were compacted under a magnetic field of 1800 kA/m followed by isostatic pressing at 150 MPa. The green compacts were sintered at 900 °C for 2 h in vacuum, followed by gas quenching, thereby obtaining pre-sintered magnet. Consequently, the pre-sintered magnets were placed in the hot-pressing vacuum machine at 800 °C and 300 MPa for 5 min and then annealed to obtain the hot-pressed pretreatment (HPP) magnets with a relatively uniform core–shell structure. The coercivity of the HPP magnet is also significantly improved compared with the conventional dual-alloy magnet.[12] At the same time, we found that the coercivity of the HPP magnets increases significantly with the increase of the annealing temperature. In this study, the microstructure of the magnets are investigated. The microstruc-

*Project supported by the Major Project of "Science and Technology Innovation 2025" in Ningbo City, China (Grant Nos. 2018B10086 and 2018B10017).

†Corresponding author. E-mail: zhengbo@nimte.ac.cn

‡Corresponding author. E-mail: gshuai@nimte.ac.cn

© 2020 Chinese Physical Society and IOP Publishing Ltd

ture factor α is studied according to the intrinsic coercivity model formula. The reasons of coercivity increase are discussed.

2. Experimental procedure

In experiment, alloys with the nominal compositions of $(NdPr)_{29}Fe_{bal.}Co_1Al_{0.1}Cu_{0.15}Ga_{0.1}B_{0.98}$ (wt%) were prepared by strip casting. The strips were subjected to hydrogen-decrepitated (HD) process and jet-milled (JM) process to obtain the powders with the average particle size of 2.8 μm. The $Tb_{90}Fe_8Al_2$ (wt%) powders with the average particle size of 2.5 μm prepared subsequently by induction melting, HD, and JM process. The Nd–Fe–B powders and the $Tb_{90}Fe_8Al_2$ powders were mixed at a ratio of 98 : 2 into the dual-alloy powders. The dual-alloy powders were compacted under a magnetic field of 1800 kA/m followed by isostatic pressing at 150 MPa. The green compacts were sintered at 900 °C for 2 h in vacuum, followed by gas quenching, thereby obtaining the pre-sintered magnets. Consequently, the pre-sintered magnets were placed in the hot-pressing vacuum machine at 800 °C and 300 MPa for five min. The pre-sintered magnets were pressed in the direction of the *c* axis. In this way, the HPP magnets were obtained. Then the HPP magnets were then annealed at 900 °C, 1000 °C, 1030 °C, and 1060 °C for 2 h and the densities are nearly the same, *i.e.*, 7.57 g/cm^3, 7.58 g/cm^3, 7.57 g/cm^3, 7.56 g/cm^3. Then those magnets were annealed at 900 °C and 500 °C for 2 h in sequence. For comparison, the original magnets of the Nd–Fe–B green compacts without $Tb_{90}Fe_8Al_2$ addition were sintered at 1060 °C and annealed at 900 °C and 500 °C for 2 h in sequence. The coercivity and remanence were respectively 14.26 kOe and 14.25 kGs (1 Gs = 10^{-4} T).

The magnets were cut by wire-electrode cutting into cylinder-shaped ones each with a size of Φ10 mm × 10 mm. The magnetic properties were measured by using a BH tracer (NIM-500 C). The microstructure feature was characterized by scanning electron microscopy (SEM) on Quanta FEG 250 with an energy dispersive spectrometer (EDS). The crystal structure and microstructure were examined by using x-ray diffraction (XRD).

3. Results and discussion

Figure 1(a) shows the demagnetization curves of the original magnet and the HPP magnets annealed at 900 °C, 1000 °C, 1030 °C, and 1060 °C, respectively. Comparing with the original magnet, the coercivity of the HPP magnet significantly increases with the annealing temperature rising. As we expected, the coercivity values of HPP magnets annealed at 900 °C, 1000 °C, 1030 °C, 1060 °C, respectively possess increments 3.4 kOe, 7.25 kOe, 8.02 kOe, 9.27 kOe. When annealed at 1060 °C, we obtain the best magnetic property, the remanence of 13.5 kGs, and the coercivity of 23.53 kOe. However, the remanence values of HPP magnets annealed at 900 °C, 1000 °C, 1030 °C, 1060 °C, decrease to different degrees, say, by 0.58 kGs, 0.32 kGs, 0.55 kGs, and 0.75 kGs. It is an interesting phenomenon that the increase of the coercivity reaches a maximum value, when the HPP magnet is annealed at 1060 °C. And the remanence tends to first increase and then decrease with annealing temperature increasing from 900 °C to 1060 °C. As we know, the density of the HPP magnet has no difference from those of magnets annealed at 900 °C to 1060 °C, the remanence trend of the HPP magnet first increases and then decreases, and the different coercivity values of the HPP magnets are mainly from different microstructural features.

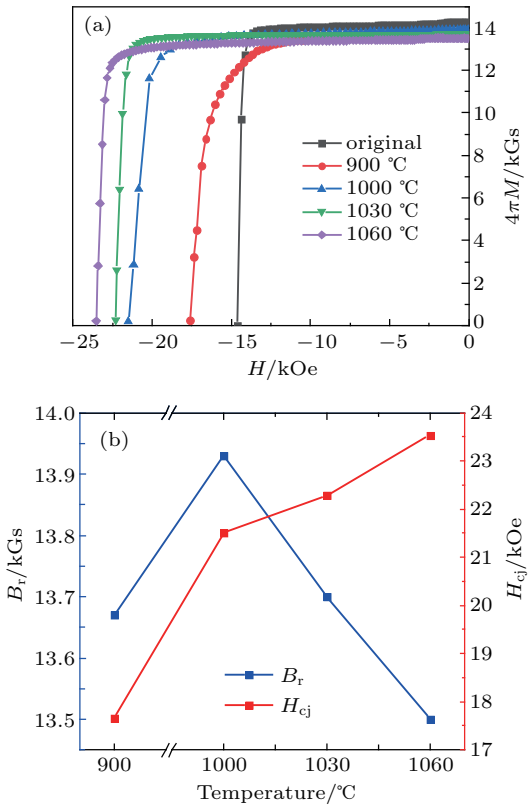


Fig. 1. (a) Demagnetization curves of original magnet and the HPP magnets annealed at 900 °C, 1000 °C, 1030 °C, and 1060 °C. (b) B_r and H_{cj} of the HPP magnets annealed at 900 °C, 1000 °C, 1030 °C, and 1060 °C.

Microstructural features of the original magnet and the HPP magnets are presented in Fig. 2. Compared with the original magnet, these HPP magnets annealed at different temperatures have obvious core–shell structure from the BSE–SEM images. In this core–shell structure, the core structure is of a 2 : 14 : 1 phase, and the shell structure is also of a 2 : 14 : 1 phase, but it is a phase after the HRE-Tb elements have partially replaced Nd.[6] Thus, the shell structure is of the $(Nd,Tb)_2Fe_{14}B$ phase. In the presence of the $(Nd,Tb)_2Fe_{14}B$ phase of the surface layer of the main phase grains, the localized magnetocrystalline anisotropy field of the surface layer of the main

phase grains will increase. Those will result in a significant increase in the coercivity of the HPP magnet.[13–15] By comparing Fig. 2(b) with Fig. 2(e), it can be seen that there are two obvious differences. One is the volume of the rich rare-earth phase (the white part in Fig. 2) gathering in triangle grain boundary. The other one is the number of irregular grains. As can be seen from Fig. 2, the volume of the rich rare-earth phase and the number of irregular grains are lower and lower with the HPP magnets annealed at 900 °C, 1000 °C, 1030 °C, and 1060 °C. It is easily understood that the rich rare-earth phase gathering in the triangle grain boundary easily dissolves the edges and corners of the irregular grains and the grain growth takes place with the temperature increasing. Although the grains of the 900 °C-annealed magnet have the angular shape, the boundaries of the grains in the magnet become smoother with the annealed temperature increasing. Therefore, the coercivity of the magnet annealed at a high temperature is higher than that of the magnet annealed at 900 °C. In addition, according to Table 1, the mass proportion of the Tb element in the shell of the main phase grains increases with the annealing temperature increasing, which is also the reason for increasing the coercivity.

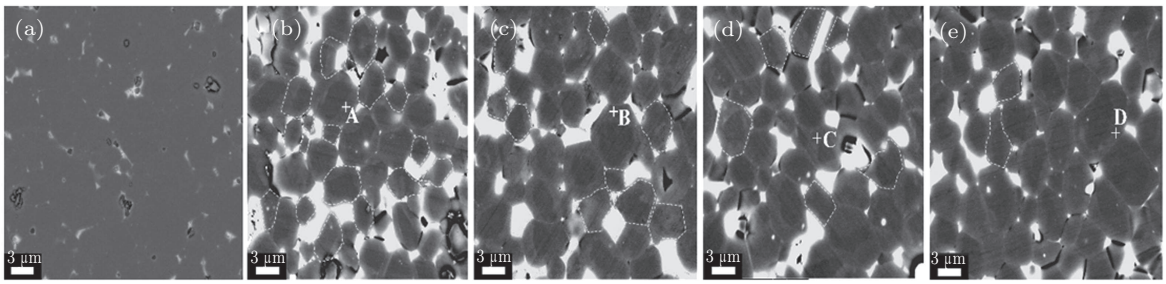


Fig. 2. BSE–SEM images of (a) original magnet and the HPP magnets annealed at (b) 900 °C, (c) 1000 °C, (d) 1030 °C, and (e) 1060 °C.

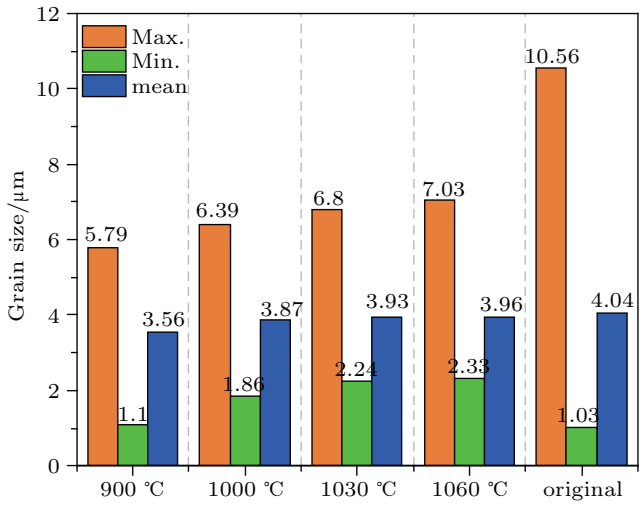


Fig. 3. Main phase grain size of original magnet and HPP magnets annealed at 900 °C, 1000 °C, 1030 °C, and 1060 °C.

There are two main reasons why the remanence of HPP magnet is lower than that of the original magnet. One reason is that the orientation degree of HPP magnet will be destroyed to some extent.[16] Another reason is that the TbFeAl entering into the main phase grains reduces the saturation magnetization of the main phase grains. In the annealing process at 1000 °C, the large grains start devouring the coarse grains to obtain an optimized texture.[17] As a result, small grains with misorientations are annexed. So the remanence of the HPP magnet at 1000 °C is higher than that of the HPP magnet at 900 °C. As shown in Table 1, the Tb content at the shell structure of grains in the HPP magnets rises with annealed temperature increasing. The replacement of Nd element in the main phase by Tb element will reduce the saturation magnetization of the main phase grains, which will cause the remanence of the magnets to decrease. This is the main reason why the remanence decreases when the HPP magnets are annealed at 1030 °C and 1060 °C.

Table 1. Rare earth content values of shell of grain in HPP magnets annealed at different temperatures.

Temperature/°C	Tb/wt%	Pr/wt%	Nd/wt%
900 (A)	3.75	4.36	21.53
1000 (B)	4.77	4.28	20.78
1030 (C)	5.34	4.2	20.67
1060 (D)	5.47	4.11	20.13

According to the image of the demagnetization curves of the magnets, it can be concluded that the remanence of the HPP magnet increases with annealing temperature rising, and the remanence changes in a range of 0.4 kGs. However, the intrinsic coercivity of the HPP magnet increases as annealing temperature increases. In order to further explain the increase in coercivity of the HPP magnet, we induce the intrinsic coercivity model expressed as[18,19]

$$H_{cj} = \alpha H_a - N_{eff} M_{s,} \tag{1}$$

where H_a in the first term on the right-hand side is the nucleation field of isolated spherical particle, α is the weakening factor of the nucleation field of the grain surface non-uniform magnetic parameter, and N_{eff} is the effective demagnetization factor of the grain interaction magnetic field in the magnet. It varies with structure, shape, and neighboring grain conditions of the grains in the magnet. The parameters α and N_{eff}

have different values for different annealing temperatures, and are generally not fixed values. Therefore, H_{cj}/M_s and H_a/M_s curves at different temperatures need plotting to determine their values.

Figure 4(a) shows the linear fitting curves of H_{cj}/M_s and H_a/M_s at different annealed temperatures of the HPP magnets. As shown in Table 2, α and N_{eff} values at different annealed temperatures are obtained. It can be seen from the fitting results that in the range of 900 °C–1000 °C, α and N_{eff} values increase with annealing temperature increasing. The main reason for the low α is that there are a number of irregular grains inside the magnets at 900 °C. The irregular grains are eliminated as the annealed temperature rises, therefore, the α at 1000 °C is improved. Because the coarse grains have a high demagnetization effect, the high N_{eff} is mainly due to the fact that the grain size of the magnet becomes larger as the annealing temperature of the magnet increases. In the range of 1000 °C–1060 °C, α and N_{eff} values both decrease with annealing temperature increasing. The main reason of low α is the microstructural defects. The reason why the value of N_{eff} decreases is that the grain boundaries become smooth and clear.[20] The combination of both α and N_{eff} makes the intrinsic coercivity of the HPP magnets increase with annealed temperature increasing.

Table 2. Microscopic magnetic fitting factor α and N_{eff} at annealing temperatures of 900 °C, 1000 °C, 1030 °C, and 1060 °C.

Sample/°C	α	N_{eff}
900	0.578	2.03
1000	0.850	3.27
1030	0.840	3.13
1060	0.825	2.98

Figure 4(b) shows that the coercivity of the magnet varies with temperature. For the magnet annealed at 900 °C, the temperature coefficient of coercivity (β) of 25 °C–125 °C is −0.51%/°C. After the magnets are annealed at 1000 °C, 1030 °C, and 1060 °C respectively, the β values of the magnets are −0.58%/°C, −0.56%/°C, and −0.53%/°C, respectively. The β value of the magnet annealed at 900 °C is the largest. This is because the average size of the grains of the magnet annealed at 900 °C is only 3.72 μm. Therefore, the β value of the magnet annealed at 900 °C is low and corresponds to the demagnetization factor N_{eff}. As can be seen from Fig. 3, the average grain size of the magnets annealed at 1000 °C, 1030 °C, and 1060 °C does not change much, but the β values of these magnets become larger as the annealing temperature rising. Since the rate of deterioration of M_s with temperature is much lower than that of H_a,[21] the lower N_{eff} is more favorable for the temperature stability of the magnet. The N_{eff} and the β of the magnets annealed under these three annealing temperatures are corresponding to each other. The essential reason for the increase in the β is that the surface of the main phase of the magnet becomes smoother.

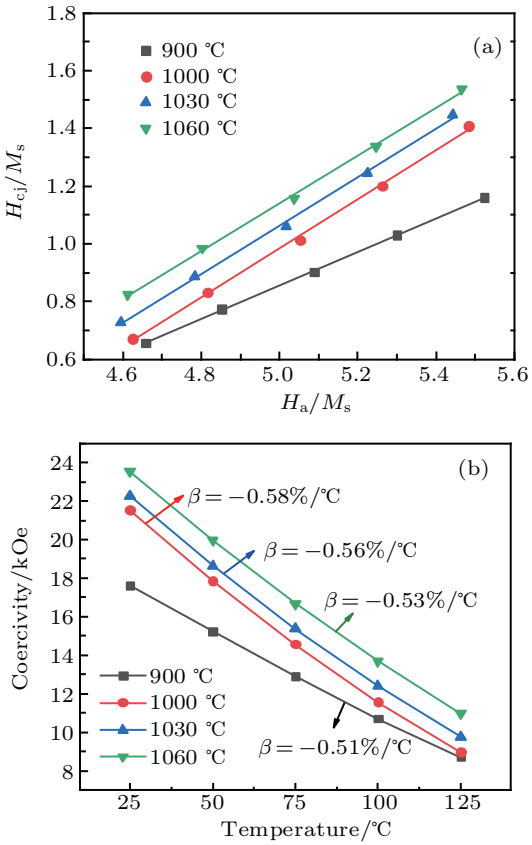


Fig. 4. (a) Linear fitting curves of H_{cj}/M_s and H_a/M_s of HPP magnets annealed at 900 °C, 1000 °C, 1030 °C, and 1060 °C. (b) Curves of the coercivity of HPP magnets *versus* temperature.

4. Conclusions

In this work, the reason why the coercivity of the HPP magnet increases is investigated. The magnet is densified after the pre-sintered magnet has experienced the hot-pressing process. The coercivity increases as the annealing temperature of the magnets rises. The coercivity is enhanced from 17.6 kOe to 23.53 kOe for the magnet annealed at 900 °C and 1060 °C. However, the remanence of the magnet fluctuates within the range of 0.4 kGs with annealing temperature changing. Microstructural analysis shows that there are many irregular grains in the magnet annealed at 900 °C, and the volume fraction of the rare earth-rich phase is high. These defects reduce the anisotropy field at the grain boundaries and easily induce the magnetization reversal nucleus to form, resulting in low coercivity. When the magnets are annealed at 1060 °C, the defects are re-paired and the surface of the grains becomes smooth, so that the coercivity is increased. According to the formula of the intrinsic coercivity model, it can be obtained that the microstructure factor α is 0.578 and 0.825 when the magnet is annealed at 900 °C and 1060 °C, respectively. Therefore, it can be concluded that the microstructure of the magnet annealed at 1060 °C is optimized, so that the

coercivity is improved.

References

[1] Gutfleisch O, Willard M A, Bruck E, Chen C H, Sankar S G and Liu J P 2011 *Adv. Mater.* **23** 821

[2] Liu W Q, Chang C, Yue M, Yang J S, Zhang D T, Liu Y Q, Zhang J X, Yi X F and Chen J W 2013 *J. Magn.* **18** 400

[3] Hirota K, Nakamura H, Minowa T and Honshima M 2006 *IEEE Trans. Magn.* **42** 2909

[4] Cao X J, Chen L, Guo S, Fan F C, Chen R J and Yan A 2017 *Scr. Mater.* **131** 24 (in Chinese)

[5] Komuro M, Satsu Y and Suzuki H 2010 *IEEE Trans. Magn.* **46** 3831

[6] Liu X B and Altounian Z 2012 *J. Appl. Phys.* **111** 07A701

[7] Tang M, Bao X, Lu K, Sun L, Li J and Gao X 2016 *Scr. Mater.* **117** 60

[8] Kong J Y, Kim T H, Lee S R, Kim H J, Lee M W and Jang T S 2015 *Met. Mater. Int.* **21** 600

[9] Sepehri-Amin H, Ohkubo T and Hono K 2010 *J. Appl. Phys.* **107** 09A745

[10] Liu W Q, Sun H, Yi X F, Liu X C, Zhang D T, Yue M S and Zhang J X 2010 *J. Alloys Compd.* **501** 67

[11] Bae K H, Kim T H, Lee S R, Namkung S and Jang T S 2012 *J. Appl. Phys.* **112** 093912

[12] Song J, Guo S, Ding G F, Chen K, Chen R J, Lee D and Yan A 2019 *J. Magn. Magn. Mater.* **469** 613

[13] Zhang T B, Zhou X Q, Yu D D, Fu Y Q, Li G J, Cui W B and Wang Q 2017 *Appl. Phys. A-Mater.* **123** 111

[14] Bae K H, Kim T H, Lee S R, NamKung S and Jang T S 2013 *IEEE Trans. Magn.* **49** 3251

[15] Ding G F, Guo S, Chen L, Di J H, Chen K, Chen R J, Lee D and Yan A 2018 *J. Alloys Compd.* **735** 1176

[16] Ju J Y, T X, Chen R J, Wang J Z, Yin W Z, Li D and Yan A 2015 *Chin. Phys. B* **24** 017504

[17] Wang Z X, Ju J Y, Wang J Z, Yin W Z, Chen R J, Li M, Jin C X, Xu Tang, Don Lee and Aru Yan 2016 *Sci. Rep.* **6** 38335

[18] Kronmüller H 1987 *Phys. Stat. Sol. (b)* **144** 385

[19] Givord D, Lu Q, Rossignol M F, Tenaud P and Viadieu T 1990 *J. Magn. Magn. Mater.* **83** 183

[20] Zhou Q, Li W, Hong Y, Zhao L Z, Zhong X C, Yu H G, Huang L L and Liu Z W 2018 *J. Rare Earth* **36** 379

[21] Hirosawa S, Matsuura Y, Yamamoto H, Fujimura S, Sagawa M and Yamauchi H 1986 *J. Appl. Phys.* **59** 873